Electronic Supplementary Material (ESI) for Analyst.

Supplementary Materials

Gaussian Clustering and Quantification of Sperm Chromatin Dispersion Test Using Convolutional Neural Network

Supplemental Table 1. Model performances with different backbone architectures. [a] The backbone name is notated as model depth and a factor *R* indicating the reduction of dimensions. Detailed model architecture is shown in **Supplemental Table 5**. [b] The time consumption in milliseconds for the neural network to process an input sized 3072×2048, the measurement of performance is made on a NVIDIA GeForce RTX 3090 GPU with 24 GiB VRAM.

Model architecture [a]	mIoU (%)	AP_{50} (%)	AP_{70} (%)	Processing time consumption for 3072×2048 input image (ms) [b]	Depth	Number of parameters
Res 10/8	68.0	82.5	34.8	7.52	10	157,247
Res 10/4	70.5	87.3	44.0	7.41	10	626,039
Res 10/2	71.6	91.9	50.0	8.54	10	2,498,279
Res 10	71.7	90.3	50.3	9.86	10	9,981,383
Res 18/2	71.7	90.0	51.8	10.36	18	4,066,919
Res 18	72.0	91.3	53.3	10.70	18	16,252,103
Res 34/2	72.1	92.2	53.0	14.54	34	6,595,815
Res 34	72.2	91.0	54.5	14.50	34	26,360,263
Res 50/2	72.2	90.3	53.5	19.61	50	8,733,543
Res 50	71.7	89.3	52.0	18.60	50	34,875,079
Res 101/2	72.4	91.5	54.5	29.10	101	13,494,631

Supplemental Table 2. The complete list of collected routine semen parameters and DFI values of semen samples included in this study.

Patient No.	DFI by SCD (%) Gaussian clustering	Concentration ($\times 10^6$/mL)	PR (%)	Motile (%)	DFI by SCSA (%)
S1	28.88	115.0	44.9	54.9	12.59
S2	28.61	39.9	30.0	34.5	21.40
S3	31.09	92.3	60.7	67.9	9.56
S4	28.47	134.3	55.5	65.7	13.28
S5	22.35	59.7	37.6	43.4	10.97
S6	16.37	97.3	44.8	51.6	12.70
S7	16.82	10.7	31.9	34.6	14.21
S8	14.04	56.0	40.8	47.2	10.45
S9	15.53	119.7	46.0	55.3	10.67
S10	15.78	55.3	52.6	57.4	11.23
S11	7.27	41.5	41.9	47.8	14.04
S12	25.67	63.1	11.7	15.4	21.40
S13	22.58	116.1	33.4	40.8	11.19
S14	17.73	65.5	18.2	23.2	13.71
S15	3.79	62.5	45.2	49.6	11.56
S16	9.54	68.9	37.7	42.4	12.46
S17	12.23	48.9	31.5	38.5	16.18
S18	9.34	66.2	23.0	28.7	11.46
S19	12.08	33.6	40.3	44.0	14.78
S20	25.32	79.5	35.9	41.7	17.20
S21	26.80	15.1	31.1	34.0	-
S22	15.89	92.8	34.0	40.2	10.86
S23	52.41	103.9	4.9	6.7	-
S24	12.41	42.4	38.7	44.8	13.94
S25	20.00	78.9	42.9	49.3	16.45
S26	31.78	30.9	24.0	28.9	15.09
S27	17.28	24.5	39.9	45.0	15.34
S28	16.69	47.7	16.7	21.0	18.22
S29	8.79	22.4	13.8	19.2	28.65
S30	20.33	150.7	49.4	59.7	11.41
S31	16.28	102.0	36.6	44.1	10.25
S32	16.61	92.7	36.8	47.8	17.90

Patient No.	DFI by SCD (%) Gaussian clustering	Concentration ($\times 10^6$/mL)	PR (%)	Motile (%)	DFI by SCSA (%)
S33	11.34	9.9	43.7	48.5	10.98
S34	13.63	101.5	16.8	20.6	19.29
S35	10.36	47.0	43.0	46.0	13.64
S36	68.79	57.0	36.0	39.0	49.79
S37	50.79	65.0	55.0	60.0	23.41
S38	15.13	49.2	20.8	25.7	5.58
S39	13.45	79.3	38.1	47.3	15.94
S40	19.17	34.6	15.6	19.2	33.33
S41	28.78	89.8	25.9	33.4	30.34
S42	16.01	52.0	63.0	65.0	13.51
S43	22.15	32.0	38.0	40.0	31.58
S44	39.86	65.0	47.0	50.0	46.61
S45	22.88	60.0	44.0	47.0	27.69
S46	36.84	31.5	10.7	12.9	51.74
S47	8.25	37.8	39.3	45.7	11.27
S48	38.77	84.3	20.1	25.9	13.78
S49	24.52	22.0	35.0	38.0	19.68
S50	12.80	50.0	46.0	49.0	14.82
S51	23.83	42.0	54.0	56.0	11.99
S52	42.84	27.0	65.0	67.0	13.46
S53	57.06	19.6	5.2	7.6	35.68
S54	43.41	30.3	28.9	31.5	25.17
S55	23.37	13.7	31.3	35.2	35.69
S56	14.69	27.0	42.0	44.0	14.64
S57	5.65	43.0	64.0	67.0	7.50
S58	18.65	42.0	44.0	47.0	21.56
S59	13.76	25.0	50.0	53.0	21.39
S60	15.77	25.0	44.0	47.0	14.93
S61	13.45	35.0	47.0	49.0	14.02
S62	16.33	30.0	41.0	44.0	15.34
S63	24.10	30.0	33.0	36.0	18.16
S64	25.14	25.0	38.0	41.0	31.31
S65	6.81	27.2	30.0	35.8	9.72
S66	7.60	7.7	33.8	39.9	14.55
S67	15.67	23.0	41.0	44.0	15.54

Patient No.	DFI by SCD (%) Gaussian clustering	Concentration ($\times 10^6$/mL)	PR (%)	Motile (%)	DFI by SCSA (%)
S68	19.35	33.0	37.0	40.0	26.17
S69	14.66	45.0	35.0	38.0	18.14
S70	8.80	34.4	20.5	26.4	8.45
S71	23.01	130.6	28.7	39.1	22.92
S72	17.41	28.0	46.0	48.0	10.91
S73	15.46	29.0	37.0	40.0	13.96
S74	11.86	50.0	53.0	55.0	10.34

Supplemental Table 3. Linear regression and correlation analysis for the relationship between DFI via SCD method, DFI via SCSA flow cytometry, and other semen parameters. Linear correlation is significant for DFI values obtained from the two methods ($p < 0.0001$, $r = 0.6017$).

(A)

DFI (SCD) % Linear regression analysis	DFI (SCSA) %	Concentration ($\times 10^6$/mL)	PR%	Motile (%)
N	72	74	74	74
Correlations				
Pearson's r	0.6058	0.1235	-0.1813	-0.2054
P value (two-tailed)	<0.0001 ****	0.2946 (ns)	0.1221 (ns)	0.0792 (ns)
Linear Regression				
Slope	0.331 to 0.632 (0.482)	n. s.	n. s.	n. s.
Y-intercept	4.554 to 11.68 (8.117)	n. s.	n. s.	n. s.
R square	0.3670	0.0152	0.0329	0.0422
F	40.59	1.114	2.447	3.170
Degree of freedoms	(1, 70)	(1, 72)	(1, 72)	(1, 72)

(B)

ROC Analysis	SCD DFI % (Gaussian clustering)	SCSA DFI %
N (Controls)	46	46
N (Asthenospermia)	28	26
Area under ROC curve		
Area under curve	0.6266 (0.4853 – 0.7678)	0.7065 (0.5725 – 0.8405)
Standard error	0.0721	0.0684
P value	0.0693	0.0038 **

Supplemental Table 4. The comparations between the predictions of ResNet 10/2 network and manual classifications by 4 laboratory technicians from different hospitals. For object detection, false negatives are missing predictions, and false positives are excess predictions. For the classification job, the true detections are then divided into TPs, TNs, FPs, and FNs. Manual results from different technicians are displayed as means ± standard deviations.

Sample No.	Cell Detections		Categories								DNA Fragmentation	
	Predictions	Manual	TP	TN	FP	FN	Missing Positives	Missing Negatives	Excess Positives	Excess Negatives	Manual DFI	Predicted DFI
I	714	737 ± 14.1	506 ± 4.2	148 ± 6.5	2 ± 3.9	48 ± 8.7	8 ± 2.5	22 ± 11.2	4 ± 0.5	6 ± 2.3	0.24 ± 0.01	0.26
II	731	739 ± 12.6	542 ± 5.0	125 ± 11.6	2 ± 3.9	49 ± 12.1	5 ± 0.7	14 ± 7.5	2 ± 1.7	6 ± 2.6	0.19 ± 0.02	0.22
III	576	576 ± 17.5	436 ± 11.7	76 ± 3.9	0 ± 0.0	50 ± 5.2	5 ± 3.0	7 ± 2.5	7 ± 8.7	4 ± 2.4	0.15 ± 0.01	0.20
IV	559	560 ± 11.6	456 ± 3.8	52 ± 11.4	1 ± 2.2	32 ± 7.9	8 ± 2.6	8 ± 3.8	4 ± 1.5	9 ± 3.6	0.11 ± 0.03	0.14
V	755	773 ± 20.5	536 ± 8.8	182 ± 2.9	6 ± 7.4	5 ± 0.4	19 ± 6.0	20 ± 11.4	16 ± 3.4	6 ± 2.4	0.27 ± 0.01	0.24
VI	753	780 ± 18.5	611 ± 4.3	117 ± 1.1	3 ± 3.9	4 ± 0.9	25 ± 9.6	13 ± 9.6	14 ± 3.0	2 ± 0.4	0.17 ± 0.01	0.15
VII	1117	1161 ± 20.2	900 ± 6.0	193 ± 1.1	4 ± 4.3	1 ± 0.4	31 ± 11.6	28 ± 8.6	16 ± 2.2	2 ± 0.9	0.20 ± 0.01	0.17
VIII	901	942 ± 25.9	762 ± 2.1	96 ± 0.4	0 ± 0.0	28 ± 0.4	40 ± 19.8	15 ± 8.9	16 ± 2.1	0 ± 0.0	0.12 ± 0.01	0.13
IX	658	682 ± 29.5	528 ± 2.7	90 ± 1.3	0 ± 0.0	22 ± 1.3	29 ± 22.1	10 ± 5.0	11 ± 2.5	5 ± 1.2	0.15 ± 0.01	0.17
X	1589	1624 ± 14.5	1220 ± 0.4	291 ± 1.3	0 ± 0.4	59 ± 1.7	20 ± 5.4	29 ± 14.1	6 ± 0.5	9 ± 1.1	0.20 ± 0.01	0.22
XI	590	605 ± 9.4	415 ± 4.7	150 ± 0.0	16 ± 4.3	2 ± 0.4	3 ± 1.0	18 ± 8.4	3 ± 0.4	2 ± 0.4	0.30 ± 0.01	0.25
XII	1175	1187 ± 6.6	1060 ± 8.6	90 ± 0.9	13 ± 4.8	4 ± 0.0	9 ± 2.3	9 ± 4.4	6 ± 3.4	0 ± 0.9	0.09 ± 0.00	0.07
XIII	405	420 ± 13.0	362 ± 1.6	30 ± 0.5	1 ± 0.4	3 ± 0.0	16 ± 11.9	6 ± 2.3	4 ± 1.2	0 ± 0.5	0.09 ± 0.00	0.07
XIV	811	828 ± 7.1	670 ± 2.6	102 ± 1.1	0 ± 0.4	31 ± 3.5	9 ± 3.1	10 ± 3.5	1 ± 2.2	4 ± 2.3	0.14 ± 0.00	0.16
XV	1067	1079 ± 7.0	838 ± 24.1	204 ± 0.9	16 ± 18.5	1 ± 0.0	4 ± 1.0	16 ± 4.4	4 ± 5.2	4 ± 0.9	0.22 ± 0.02	0.18
Total	12401	12692 ± 64.2	9841 ± 32.0	1946 ± 18.4	66 ± 22.5	339 ± 18.2	230 ± 36.8	225 ± 30.5	115 ± 12.7	61 ± 6.9	-	-

Supplemental Table 5. Detailed network architectures for models in this study. [a] The convolution layer is denoted as (input dimension, output dimension, size, stride), batch normalization as (size, stride), and transpose convolutions as (kernel size, padding, output padding). [b] *D* is by default 64, in networks with reduced dimensions (for example ResNet 10/2, *R* = 2), *D* = 64 / *R*.

	Input Shape [b]	Output Shape [b]	Layers	Model Architecture [a]				
				ResNet 10	ResNet 18	ResNet 34	ResNet 50	ResNet 101
Pre-process Layers								
'preprocess.0'	(1, 512, 512)	(D, 256, 256)	Conv	(1, D, 7, 2)	(1, D, 7, 2)	(1, D, 7, 2)	(1, D, 7, 2)	(1, D, 7, 2)
'preprocess.1'	(D, 256, 256)	(D, 256, 256)	BatchNorm					
ReLU	(D, 256, 256)	(D, 256, 256)	ReLU					
MaxPool	(D, 256, 256)	(D, 128, 128)	MaxPool	(3, 2)	(3, 2)	(3, 2)	(3, 2)	(3, 2)
Backbone Layers								
'layer1'	(D, 128, 128)	(D, 128, 128)		1 × Basic Block	2 × Basic Block	3 × Bottleneck	3 × Bottleneck	3 × Bottleneck
'layer2'	(D, 128, 128)	(2D, 64, 64)		1 × Basic Block	2 × Basic Block	4 × Bottleneck	4 × Bottleneck	4 × Bottleneck
'layer3'	(2D, 64, 64)	(4D, 32, 32)		1 × Basic Block	2 × Basic Block	6 × Bottleneck	6 × Bottleneck	23 × Bottleneck
'layer4'	(4D, 32, 32)	(8D, 16, 16)		1 × Basic Block	2 × Basic Block	3 × Bottleneck	3 × Bottleneck	3 × Bottleneck
'deconvolutionlayers.0'	(8D, 16, 16)	(4D, 32, 32)	ConvTranspose	(4, 1, 0)	(4, 1, 0)	(4, 1, 0)	(4, 1, 0)	(4, 1, 0)
'deconvolutionlayers.1'	(4D, 32, 32)	(4D, 32, 32)	BatchNorm					
ReLU	(4D, 32, 32)	(4D, 32, 32)	ReLU					
'deconvolutionlayers.3'	(4D, 32, 32)	(4D, 64, 64)	ConvTranspose	(4, 1, 0)	(4, 1, 0)	(4, 1, 0)	(4, 1, 0)	(4, 1, 0)
'deconvolutionlayers.4'	(4D, 64, 64)	(4D, 64, 64)	BatchNorm					
ReLU	(4D, 64, 64)	(4D, 64, 64)	ReLU					
'deconvolutionlayers.6'	(4D, 64, 64)	(4D, 128, 128)	ConvTranspose	(4, 1, 0)	(4, 1, 0)	(4, 1, 0)	(4, 1, 0)	(4, 1, 0)
'deconvolutionlayers.7'	(4D, 128, 128)	(4D, 128, 128)	BatchNorm					
ReLU	(4D, 128, 128)	(4D, 128, 128)	ReLU					
Terminal Layers								
Center prediction								
'heatmap.0'	(4D, 128, 128)	(2D, 128, 128)	Conv	(4D, 2D, 3, 1)	(4D, 2D, 3, 1)	(4D, 2D, 3, 1)	(4D, 2D, 3, 1)	(4D, 2D, 3, 1)
ReLU	(2D, 128, 128)	(2D, 128, 128)	ReLU					
'heatmap.2'	(2D, 128, 128)	(1, 128, 128)	Conv	(2D, 1, 1, 1)	(2D, 1, 1, 1)	(2D, 1, 1, 1)	(2D, 1, 1, 1)	(2D, 1, 1, 1)
Offset prediction								
'offset.0'	(4D, 128, 128)	(2D, 128, 128)	Conv	(4D, 2D, 3, 1)	(4D, 2D, 3, 1)	(4D, 2D, 3, 1)	(4D, 2D, 3, 1)	(4D, 2D, 3, 1)
ReLU	(2D, 128, 128)	(2D, 128, 128)	ReLU					
'offset.2'	(2D, 128, 128)	(2, 128, 128)	Conv	(2D, 2, 1, 1)	(2D, 2, 1, 1)	(2D, 2, 1, 1)	(2D, 2, 1, 1)	(2D, 2, 1, 1)
Regression prediction								

‘regr.0’	(4D, 128, 128)	(2D, 128, 128)	Conv	(4D, 2D, 3, 1)	(4D, 2D, 3, 1)	(4D, 2D, 3, 1)	(4D, 2D, 3, 1)	(4D, 2D, 3, 1)
ReLU	(2D, 128, 128)	(2D, 128, 128)	ReLU					
‘regr.2’	(2D, 128, 128)	(4, 128, 128)	Conv	(2D, 4, 1, 1)	(2D, 4, 1, 1)	(2D, 4, 1, 1)	(2D, 4, 1, 1)	(2D, 4, 1, 1)

Supplemental Figure 1. Learning curve analysis and model performance when (a) including fewer training images and (b) decreased scale of random rotation in data augmentation. The performance saturate at 50% size of training set and 8× rotation.

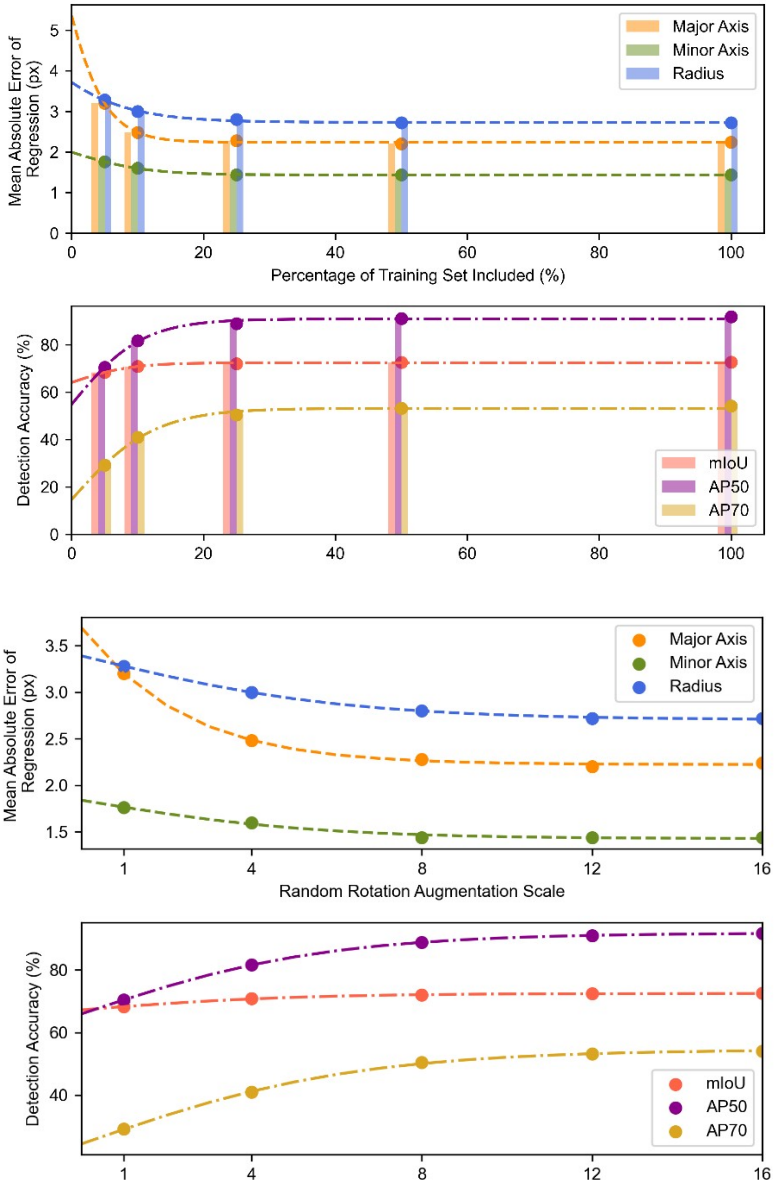

Supplemental Figure 2. A. The linear correlation between DFI values obtained from SCD and SCSA flow cytometry. Detailed statistics are shown in Table 3. B. The ROC curve for SCD and SCSA methods for differentiating normal semen samples and samples that are considered asthenospermia (PR < 32% or motile percentile < 40%) C. The significance of SCD DFI% difference between normal and asthenospermia samples, for gaussian clustering method and static thresholding. * Label 'T n': sperms with relative halo radius < n% is regarded as DNA fragmented.

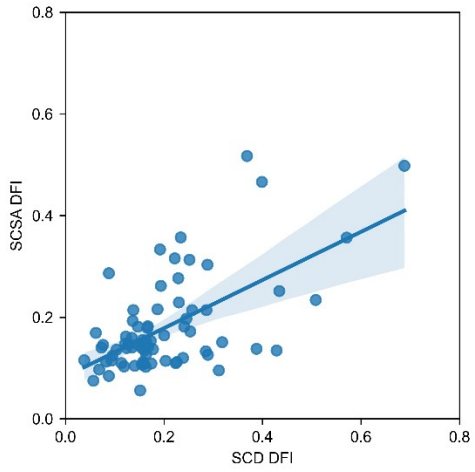

(A)

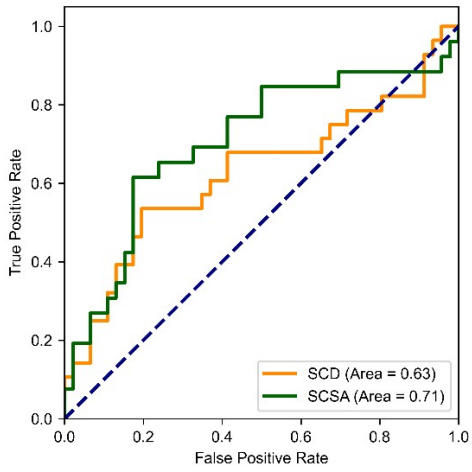

(B)

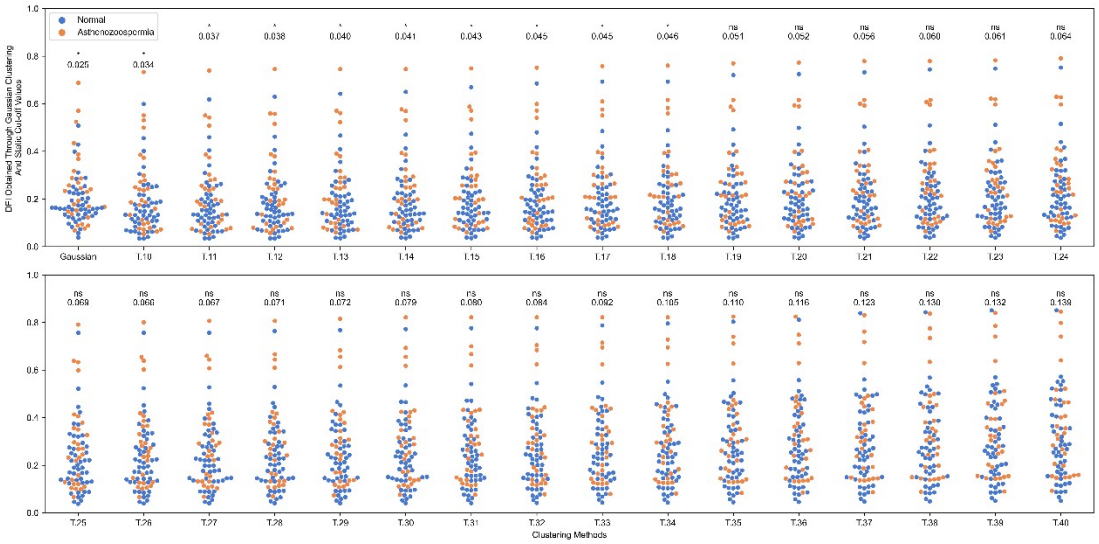

(C)

Supplemental Figure 3. A. The user interface of SCD automation software. B. Sample and image management. The image repository can be loaded and saved to the hard disk. C. Automatic prediction of the selected sample image. The distribution is analyzed and the detailed prediction markers can be displayed superimposed to the original image. D. Technicians can revise the predicted results and save changes to the repository.

(A)

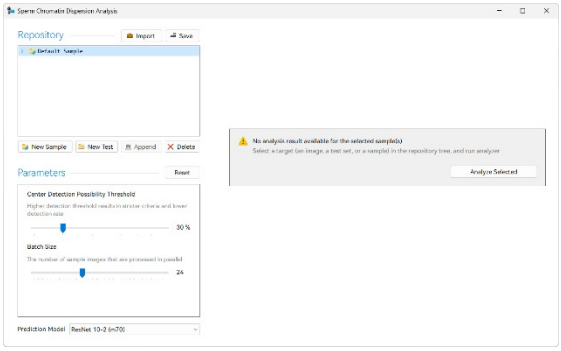

(B)

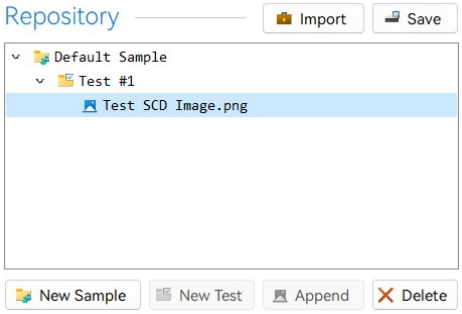

(C)

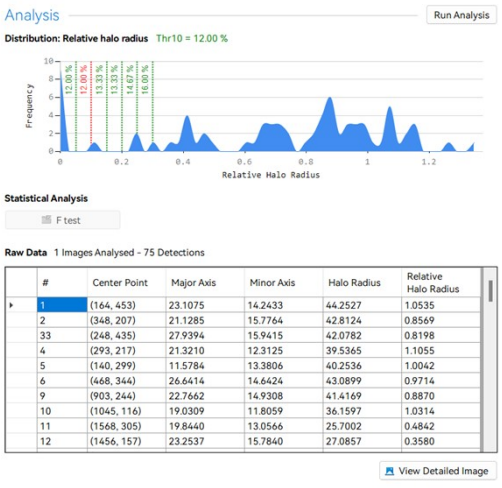

(D)

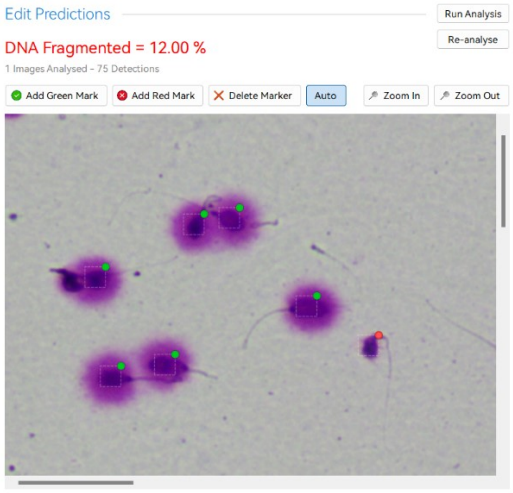

Supplemental Movie 1. The procedure of annotating SCD dataset by SCDLabel utility software. (See Additional Files)
Supplementary Movie 1 - SCD Annotating.mp4

Data and Code Availability: The data underlying this study are openly available in Mendeley Data at Zheng Y, Lei Z (2023) “Sperm chromatin dispersion bright field images”, Mendeley Data, V1, doi: 10.17632/p3ntt2z294.1, and source code is also available on https://github.com/Xornent/scd-resnet/.